

Analysis of Triterpenoid Saponins Reveals Insights into Structural Features Associated with Potent Protein Drug Enhancement Effects

Xue-Wei Cao, Fu-Jun Wang,* Oi-Wah Liew, Ye-Zhou Lu, and Jian Zhao*

Cite This: *Mol. Pharmaceutics* 2020, 17, 683–694

Read Online

ACCESS |



Metrics & More



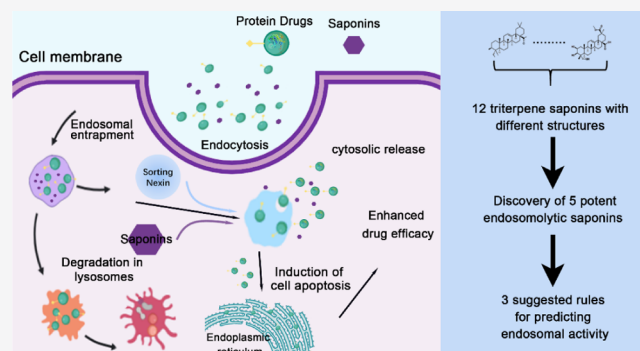
Article Recommendations



Supporting Information

ABSTRACT: Plant-based saponins are amphipathic glycosides composed of a hydrophobic aglycone backbone covalently bound to one or more hydrophilic sugar moieties. Recently, the endosomal escape activity of triterpenoid saponins has been investigated as a potentially powerful tool for improved cytosolic penetration of protein drugs internalized by endocytic uptake, thereby greatly enhancing their pharmacological effects. However, only a few saponins have been studied, and the paucity in understanding the structure–activity relationship of saponins imposes significant limitations on their applications. To address this knowledge gap, 12 triterpenoid saponins with diverse structural side chains were screened for their utility as endosomolytic agents. These compounds were used in combination with a toxin (MAP30-HBP) comprising a type I ribosome-inactivating protein fused to a cell-penetrating peptide. Suitability of saponins as endosomolytic agents was assessed on the basis of cytotoxicity, endosomal escape promotion, and synergistic effects on toxins. Five saponins showed strong endosomal escape activity, enhancing MAP30-HBP cytotoxicity by more than 10^6 to 10^9 folds. These saponins also enhanced the apoptotic effect of MAP30-HBP in a pH-dependent manner. Additionally, growth inhibition of MAP30-HBP-treated SMMC-7721 cells was greater than that of similarly treated HeLa cells, suggesting that saponin-mediated endosomolytic effect is likely to be cell-specific. Furthermore, the structural features and hydrophobicity of the sugar side chains were analyzed to draw correlations with endosomal escape activity and derive predictive rules, thus providing new insights into structure–activity relationships of saponins. This study revealed new saponins that can potentially be exploited as efficient cytosolic delivery reagents for improved therapeutic drug effects.

KEYWORDS: saponins, endosomal escape enhancers (EEEs), glycosylated triterpenoid, ribosome-inactivating proteins (RIPs), cytosolic drug delivery, drug release



1. INTRODUCTION

Since the first application of the cell-penetrating peptide (CPP) transactivating transcriptional activator for the trans-membrane transport of biomacromolecules, great progress has been achieved in drug delivery technology.¹ To date, a variety of CPPs have been developed and optimized for enhanced intracellular delivery of therapeutic agents. Generally, protein drugs internalize into cells by receptor-mediated endocytosis via caveolin-/clathrin-dependent or independent pathways and are eventually sequestered in endosomes.^{2–4} However, only about 10% of these proteins are released into the cytosol to exert their bioactivity,^{5,6} while most are trapped in endosomes and eventually degraded in lysosomes.^{7,8} Hence, endocytosed protein drugs are usually not very effective and require relatively high concentrations to exert their pharmacological effects, with the attendant problem of causing more unwanted side effects. Thus, lysosomal trapping of internalized protein drugs severely limits their potential clinical applications. Therefore, it is essential to discover effective strategies that

enhance the cytosolic release of protein drugs from endosomes or lysosomes to maximize their bioactivity.

Interestingly, this problem has long been recognized in nature as exemplified by the way with which viruses penetrate cells and subsequently gain access to the cytoplasm via inbuilt endosomal escape domains (EEDs) in some of their proteins, such as the subunit of the influenza virus hemagglutinin-2 subunit (HA2).⁹ These natural EEDs have been fused with protein drug molecules to facilitate cytosolic entry for enhanced therapeutic or toxicity effects. For example, a 25 amino acid small peptide from the N-terminus of protein G of the vesicular stomatitis virus envelope (KFT25) has been shown to improve the cytotoxicity of ricin toxin A (RTA)

Received: November 9, 2019

Revised: January 3, 2020

Accepted: January 8, 2020

Published: January 8, 2020



chain about 20 times.¹⁰ HA2 markedly improved the cytosolic entry of an endocytosed CPP-/HA2-fused reporter protein¹¹ and the ability of p53 to induce cell apoptosis.¹² Compared with the limited enhancement effects of EEDs, another class of promising small-molecule compounds known as endosomal escape enhancers (EEEs) have been demonstrated to elicit hundred to thousand-fold enhancement of protein drugs.¹³ For example, coadministration of chemical EEEs including cyclosporin A,¹⁴ retinoic acid,¹⁵ and monensin^{16–19} improved the cytotoxicity of pseudomonas exotoxin and RTA chain about 4–12 000 times. The well-known lysosomotropic amine, chloroquine (CQ), increased the toxicity of a RTA-fused immunotoxin by approximately 2500 folds.²⁰ In addition, CQ also augmented the cytotoxicity of gelonin, granzyme B, and saporin by 3–15 times.²¹ Our previous work provided evidence for the EEE activity of cyclosporin A whereby the enhanced anticancer effect of MAP30-S3 was obtained with its cytosolic release as deduced from its diffused distribution in the cytoplasm.²²

Of the structurally different EEEs, coadministration of a special class of EEEs comprising plant-derived glycosylated triterpenoids has been found to improve the pharmacological effects of protein drugs by more than 10 000 folds.²³ Glycosylated triterpenoids are a class of saponins comprising a triterpene aglycone to which one or more sugar moieties are attached, giving rise to a diversity of structural variations (reviewed in 24). These secondary plant metabolites are thought to play a role in defense against herbivores and pathogens.²⁵ The most common glycosylated triterpenoids are tetracyclic triterpenes (cucurbitane, dammarane, and lanostane) and pentacyclic triterpenoids (oleanane and lupine). Among these triterpenoids, the striking efficacy of oleanane-type triterpenoid saponins in enhancing the endosomal escape of protein drugs makes it an extremely attractive candidate EEE for further therapeutic development. Oleanane-type triterpenoid saponins are glycosides composed of a pentacyclic hydrophobic backbone and a series of covalently bound hydrophilic sugar chains.²⁶ Because of their unique amphiphilic structures, oleanane saponins can exert extremely strong endosomal escape activity. For instance, Saponinum album (a saponin extract of *Gypsophila paniculata* L.) could enhance the cytotoxicity of saporin-derived target toxin by more than 10 000 times.²⁷ Many studies have demonstrated the strong endosomal escape activity of saponins, which has driven concerted efforts to elucidate structure–function relationships.^{24,28–30} An analysis of SO1861 revealed the contribution of C-4, C-28, and C-16 side chains to its endosomal escape activity.³¹ Another study investigated the role of charge in saponin-mediated endosomal escape and showed that saponins with different relative electrophoretic mobilities exerted distinct endosomal escape activity.³² Böttger et al. showed that saponins of molecular mass greater than 1600 g/mol with branched trisaccharide at C-3 containing a glucuronic acid and branched sugar chains attached at C-28 are necessary for activity.³³ To date, current data providing a glimpse of structure–function relationships are based on the studies of a limited number of saponins (such as SO1861) with similar structures (MW \geq 1.6 kD). In fact, the diversity of the side-chain structures and biological activity of oleanane-type saponins make the relationship between the structure and activity highly complex. Thus, it is imperative to further probe structure–activity relationships to elucidate preferred structural features that portend enhanced endosomal escape ability.

This will aid further exploration and utilization of the unique functions of these saponins.

In this study, we selected 12 oleanane-type triterpenoid saponins extracted from different medicinal herbs with diverse structural side chains and assessed their efficacy as endosomolytic agents in synergy with a cytotoxic antitumor protein MAP30 fused to HBP, a CPP derived from heparin-binding epidermal growth factor (HB-EGF) (the recombinant protein was named MAP30-HBP). The utility of these saponins was evaluated based on the following three aspects: modulation of intracellular distribution of endocytosed proteins, enhancement of MAP30-HBP cytotoxicity, and induction of cellular apoptosis. Five of the 12 saponins were found to exhibit strong endosomal escape activity with significant enhancement of MAP30-HBP cytotoxicity. From the results, we postulated preliminary rules for predicting the level of endosomal escape activity of a particular saponin on the basis of its structural hydrophobicity. Our study elucidates the mechanisms of saponin-mediated endosomal escape to pave the way for improved cytosolic drug release after intracellular delivery.

2. EXPERIMENTAL SECTION

2.1. Chemicals and Reagents. *Quillaja* bark saponin (QBS) was purchased from the Sangon Biotech with approximate 25% sapogenin. The components of QBS were identified using liquid chromatography (LC)–mass spectrometry (MS) (ThermoFisher Scientific) and are listed in Table S1 and Figure S1. Sodium aescinate, macranthoidin A, esculentoside A, and dipsacoside B were purchased from the Bokachem (Shanghai) with 98% (w/w) purity as confirmed by high-performance LC (HPLC). Saikosaponin A, saikosaponin C, saikosaponin D, and phytolaccagenin were purchased from Shanghai R&D Center for Standardization of Chinese Medicines (Shanghai) with 98% (w/w) purity as confirmed by HPLC. Asperosaponin VI, asiaticoside, and glycyrrhizic acid were purchased from Eybridge (Shanghai) with 98% (w/w) purity as confirmed by HPLC. Ginsenoside Ro (with 98% [w/w] purity as confirmed by HPLC) was a gift from Dr Zhengtao Wang, Institute of Chinese Materia Medica, Shanghai University of Traditional Chinese Medicine. All saponins were dissolved in dimethyl sulfoxide (DMSO) to generate a 20 mg/mL stock solution and stored at -20°C . The final concentration of DMSO was <1% in all experiments. The systematic names of all the saponins are listed in Table S2.

2.2. Plasmid Constructs and Protein Preparation. Two recombinant proteins derived from the plasmids MAP30-HBP-pET28b and enhanced green fluorescent protein (EGFP)-HBP-pET28a were purified according to our previous reports.^{22,34} Briefly, the plasmids were transformed into *Escherichia coli* BL21 (DE3) competent cells (CWBI0, China), and the cells were cultured in Luria Broth medium with kanamycin (50 $\mu\text{g/mL}$). MAP30-HBP and EGFP-HBP expression were induced with 0.5 mM isopropyl- β -D-1-thiogalactopyranoside (Sangon Biotech, Shanghai, China) at 16°C for 16–18 h. *E. coli* cells were harvested by centrifugation at 3000 rpm for 20 min at 4°C . Cells were then resuspended in Tris–HCl buffer (20 mM Tris–HCl, 0.5 M NaCl, 5% glycerol, pH 8.5), followed by ultrasonication in an ice bath. After centrifugation at 12 000 rpm for 20 min at 4°C , supernatants were carefully collected, and recombinant proteins were purified by Ni-NTA affinity chromatography (IMAC), followed by dialysis against 20 mM Tris–HCl/0.5 M NaCl/5% glycerol (pH 7.2) for about 6 h. Purified proteins

were stored at -80°C . The concentrations of proteins were quantified by the bicinchoninic acid protein assay (Dingguo Biotech, China).

To prepare fluorescein isothiocyanate (FITC)-labeled proteins, IMAC-purified MAP30-HBP was dialyzed against a $\text{Na}_2\text{CO}_3\text{--NaHCO}_3$ (pH 9.0) buffer solution. FITC (Sangon, China) was dissolved in DMSO ($30\text{ }\mu\text{g}$ of FITC per 1 mg protein). MAP30-HBP was mixed with FITC for 8 h at 4°C in the dark. The treated proteins were then dialyzed against phosphate-buffered saline (PBS) (pH 7.2) for about 8 h to remove unbound FITC. Prepared proteins were analyzed using sodium dodecyl sulfate polyacrylamide gel electrophoresis (Figure S2).

2.3. Cell Lines and Cell Culture. HeLa (human cervical cancer cells), MGC-803 (human gastric cancer cells), and SMMC-7721 (human hepatoma cells, referred to as SMMC for short) cell lines were purchased from the Institute of Biochemistry and Cell Biology, Chinese Academy of Sciences (Shanghai, China). Cells were cultured at 37°C in an atmosphere of 5% CO_2 in RPMI-1640 medium (Corning, USA) containing streptomycin (100 U/mL), penicillin ($100\text{ }\mu\text{g/mL}$) (HyClone, USA), and 10% fetal bovine serum (GEMINI, California, USA).

2.4. Confocal and Fluorescence Microscopy. HeLa cells (1.0×10^4 cells/well) were seeded in 24-well plates (Costar, USA) and cultured for approximately 12 h until 50% confluent. Subsequently, the cells were treated with $5\text{ }\mu\text{M}$ FITC-labeled MAP30-HBP or EGFP-HBP recombinant proteins in combination with 1 of 12 saponins ($10\text{ }\mu\text{g/mL}$ saponin, $25\text{ }\mu\text{M}$ sodium aescinate, $100\text{ }\mu\text{M}$ esculentoside A, $100\text{ }\mu\text{M}$ phytolaccagenin, $10\text{ }\mu\text{M}$ saikosaponin A, $25\text{ }\mu\text{M}$ saikosaponin C, $5\text{ }\mu\text{M}$ saikosaponin D, $100\text{ }\mu\text{M}$ dipsacoside B, $100\text{ }\mu\text{M}$ asperosaponin VI, $100\text{ }\mu\text{M}$ asiaticoside, $100\text{ }\mu\text{M}$ glycyrrhizic acid, and $100\text{ }\mu\text{M}$ macranthoidin A) for 2 h . Lysosomes were then labeled with LysoTracker Red (Beyotime Biotechnology, Haimen, China) according to the manufacturer's protocol, which were visualized as red signals, followed by three rinses with PBS. Cells were then fixed in 4% paraformaldehyde (Sango, Shanghai, China) for 20 min at room temperature. Finally, $4',6\text{-diamidino-2-phenylindole}$ (DAPI) (Beyotime Biotechnology, Haimen, China) was added to stain the cells according to the manufacturer's protocol, which were visualized as blue signals. Intracellular fluorescent signals were captured by confocal microscopy (Nikon, Tokyo, Japan), and colocalization of the recombinant protein with lysosome was assessed by calculating Person's correlation coefficients using Image-Pro Plus (IPP) software 6.0 (Medical Cybernetics, North Carolina, USA).

2.5. Cell Viability Assay. The cell inhibition effect of different saponins on HeLa and SMMC-7721 cells was examined using the 3-(4,5-dimethylthiazol-2-yl)-2,5-diphenyltetrazolium bromide (MTT) assay. In summary, cells (4×10^3 cells/well) were seeded in 96-well plates and incubated at 37°C for 12 h , followed by treatment with different concentrations of saponins for 24 h . The cells were further treated with medium containing $20\text{ }\mu\text{L}$ of 5 mg/mL MTT (Sango, Shanghai, China) solution for 4 h at 37°C . Next, the culture medium was carefully removed, and $150\text{ }\mu\text{L}$ of DMSO (Titan, China) was added to dissolve the crystals, and the absorbance value was determined using a microplate reader (Thermo Scientific, USA) at 492 nm .

The MTT assay was used to assess the synergistic effect of different saponins on MAP30-HBP cytotoxicity. MAP30-HBP

($500, 100, 20, 4, 0.8\text{ nM}$) was added to cells after cell adherence with or without the addition of different saponins at specific concentrations. Cells treated with dialysis buffer (20 mM Tris-HCl/ 0.5 M NaCl/ 5% glycerol) with or without saponins served as controls. The MTT assay as described above was then performed.

To test whether CQ could affect the endosomal escape activity of different saponins, MAP30-HBP ($500, 100, 20, 4, 0.8\text{ nM}$) in combination with one saponin ($10\text{ }\mu\text{g/mL}$ saponin, $10\text{ }\mu\text{M}$ sodium aescinate, $100\text{ }\mu\text{M}$ esculentoside A, $10\text{ }\mu\text{M}$ saikosaponin A, or $5\text{ }\mu\text{M}$ saikosaponin D) was added to cells after cell adherence with or without the presence of $100\text{ }\mu\text{M}$ CQ. The subsequent steps were the same as described above.

2.6. Apoptosis and Membrane Integrity Assay. SMMC-7721 cells (1.0×10^6 cells/well) were seeded on six-well plates (Costar, USA) and cultured for approximately 12 h until 60% confluent, and then 5 nM MAP30-HBP and one of different saponins or saponins alone at required concentrations ($10\text{ }\mu\text{g/mL}$ saponin, $25\text{ }\mu\text{M}$ sodium aescinate, $100\text{ }\mu\text{M}$ esculentoside A, $100\text{ }\mu\text{M}$ phytolaccagenin, $10\text{ }\mu\text{M}$ saikosaponin A, $25\text{ }\mu\text{M}$ saikosaponin C, $5\text{ }\mu\text{M}$ saikosaponin D, $100\text{ }\mu\text{M}$ dipsacoside B, $100\text{ }\mu\text{M}$ asperosaponin VI, $100\text{ }\mu\text{M}$ asiaticoside, $100\text{ }\mu\text{M}$ glycyrrhizic acid, and $100\text{ }\mu\text{M}$ macranthoidin A) were added to SMMC-7721 cells. After incubation for 12 h , cells were detached using ethylenediaminetetraacetic acid-free trypsin and harvested by centrifugation at 1000 rpm for 5 min . Cells were resuspended and washed twice with $500\text{ }\mu\text{L}$ of PBS and finally resuspended in $100\text{ }\mu\text{L}$ of binding buffer containing $5\text{ }\mu\text{L}$ of 7-AAD and Annexin V-PE according to the manufacturer's protocol (Sony biotech, Japan). The cells were then stored in the dark at room temperature for 30 min . Prior to detection, another $400\text{ }\mu\text{L}$ of binding buffer was added to cells, followed by flow cytometry (Becton Dickinson, New Jersey, USA). The apoptosis rate was calculated using FlowJo 6.0 software.

2.7. Data and Materials Availability. The gene expression dataset (accession number GSE57083) was downloaded from the Gene Expression Omnibus (GEO) and analyzed for differentially expressed genes in a panel of cells.³⁵

2.8. Data and Statistical Analysis. All data were obtained from at least three independent experiments and are presented as mean \pm standard deviation. Statistical analysis of the data was calculated using GraphPad Prism 6.0 software (San Diego, USA). Unpaired student's *t*-test was used to determine the significance between the control groups and the saponin-treated groups. $P < 0.05$ was considered to be statistically significant.

3. RESULTS

3.1. Determination of the Effects of Different Saponins on Cell Viability, Apoptosis, and Membrane Integrity. The structure of glycosylated triterpenoids manifests wide variations in the triterpene backbone and attached sugar side chains. To shed light on structure–activity relationships, 12 triterpenoid saponins (Table 1) of diverse side-chain features were tested for their ability to elicit endosomal escape. Figure 1 shows the typical aglycone structure of oleanane-type triterpenoid saponins and the broad array of side-chain structures. The selected saponins have different side-chain lengths at C-3 and ester chains at C-28, structural features that are expected to influence their respective endosomal escape activity. Briefly, the noncytotoxic/membrane impermeable concentration (NCMIC) of

Table 1. List of 12 Saponins and Their NCMICs

name	working concentration	maximum NCMIC ^a
QBS	4 $\mu\text{g/mL}$	10 $\mu\text{g/mL}$
sodium aescinate	10 μM	25 μM
saikosaponin A	5 μM	10 μM
saikosaponin C	25 μM	50 μM
saikosaponin D	2 μM	5 μM
esculentoside A	50 μM	100 μM
phytolaccagenin	50 μM	100 μM
dipsacoside B	50 μM	100 μM
macranthoidin A	50 μM	100 μM
asperosaponin VI	50 μM	100 μM
asiaticoside	50 μM	100 μM
glycyrrhizic acid	50 μM	100 μM

^aTested only in HeLa and SMMC-7721 cells.

each saponin was first determined. Each saponin below its NCMIC was then used in conjunction with the cytotoxic agent MAP30-HBP on different cell types.

To determine the NCMIC, the effects of each saponin on cell viability of HeLa and SMMC-7721 cancer cells after 24 h of incubation were examined using the MTT assay. As shown in Figure 2A and Supporting Information, Figures S3A and S4, the saponins showed varying degrees of cytotoxicity to the cells. For saponins that display mild cytotoxicity such as esculentoside A and saikosaponin C, the working concentration used was 50% of its NCMIC. In the case of saponins where significant cytotoxicity was observed, the working concentration was 40% of its NCMIC. The NCMIC and selected working concentrations of each saponin are summarized in Table 1.

To validate the selected working concentrations of each saponin, an Annexin-V/7-AAD apoptosis detection kit was used, and the results are shown in Figures 2B and S3B. Our

study showed that all saponins did not induce significant apoptosis at the working concentrations listed in Table 1. Previous studies have revealed the ability of saponins to disrupt membrane integrity because of their amphiphilic properties³⁶ and could confound interpretation of results on endosomal escape. 7-AAD is a membrane-impermeable dye and could also be used to assess membrane integrity.^{37,38} Our results demonstrated that no significant 7-AAD positive cells were detected in saponin-treated cells compared to blank controls (Figure 2C). At the same time, the presence of saponins did not significantly affect the internalization efficiency of EGFP fused with a CPP, HBP (EGFP-HBP) (Figure 2D). This is in agreement with previous studies that saponins had no effect on cell membrane integrity. When used at the working concentrations listed in Table 1, all 12 saponins had no detectable effect on cell viability, apoptosis, and membrane integrity. Hence, these concentrations were used for endosomal escape analysis in subsequent experiments.

3.2. Saponins Do Not Affect the Endocytic Efficiency but Weakly Inhibits Colocalization of Endocytic Proteins with Lysosomes. The recombinant toxin MAP30-HBP was used as a model protein to evaluate the endosomal escape properties of each saponin. MAP30 is a type I ribosome-inactivating protein (RIP) derived from *Momordica charantia* that inhibits HIV-1 viral replication and cancer cell growth.^{39,40} HBP is a human-derived CPP studied in our laboratory and has been shown to effectively transport proteins into cancer cells and when fused with MAP30 can enhance the cytotoxicity of the toxin.³⁴ In this study, 5 μM FITC-labeled MAP30-HBP was incubated with HeLa cells for 2 h with or without saponins, while the lysosomes in the tested cells were simultaneously labeled by LysoTracker. A confocal laser scanning microscope was used to observe the translocation efficiency of MAP30-HBP, its cellular distribution, and colocalization with lysosomes. As shown in Figures 3A and

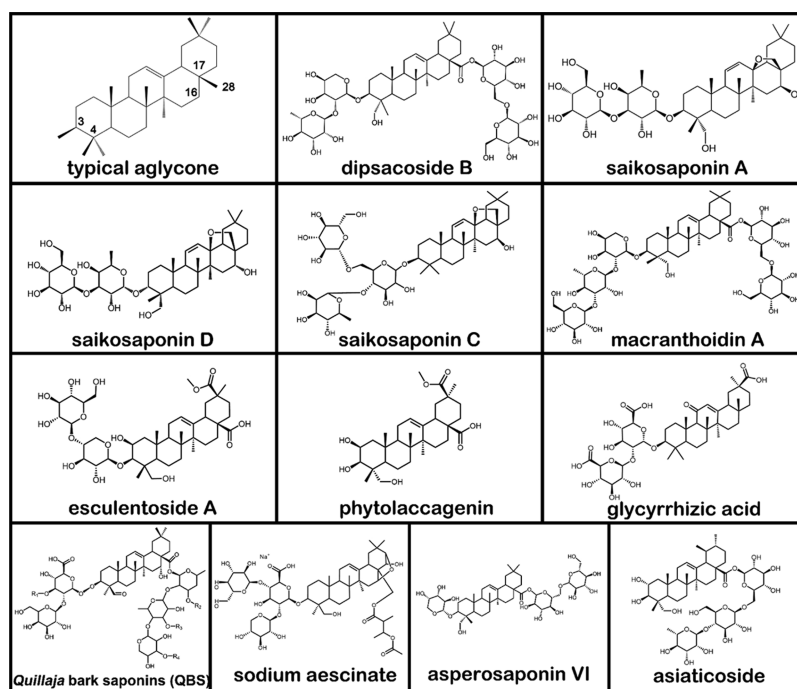


Figure 1. Structures of oleanane-type triterpenoid saponins. The typical structure of aglycone and all the structures of 12 saponins. QBS is a mixture; the structure listed here is only one of the typical structures. R1–R4 represent hydrogen or a carbohydrate group.

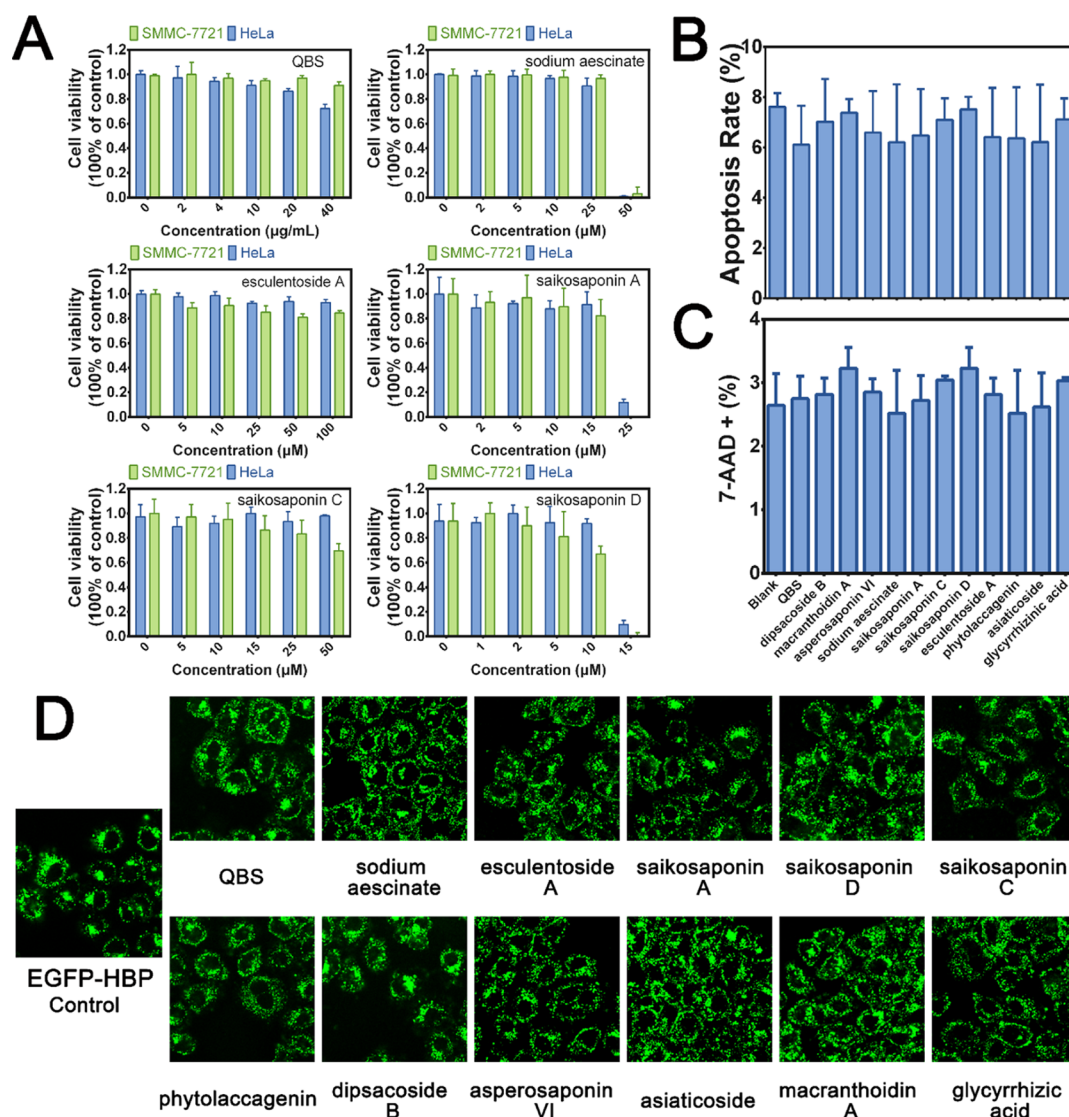


Figure 2. Effects of saponins on cells as assessed by cell viability (cytotoxicity), apoptosis, and membrane integrity. (A) HeLa and SMMC-7721 cells were incubated with different concentrations of saponins for 24 h. Cell viability was measured using the MTT assay, and data were plotted using GraphPad 6.0 software (error bars represent the mean \pm SD, $N = 5$). (B) SMMC-7721 cells were incubated with different saponins at NCMIC for 12 h. Cells were collected and stained with Annexin V-PE/7-AAD, followed by flow cytometry. The apoptosis rate (Q2 + Q3) was calculated by Flow Jo software and plotted by GraphPad 6.0 software. Data were presented as mean \pm SD, $N = 3$. (C) The percentage of 7-AAD positive cells (Q1 + Q2) was calculated by Flow Jo software and plotted by GraphPad 6.0 software. Data were presented as mean \pm SD, $N = 3$. (D) HeLa cells were incubated with EGFP-HBP (5 μ M) and different saponins for 2 h, and images were captured using confocal microscopy.

SS, treatment with saponins or CQ (a lysosomotropic amine) did not significantly affect the internalization efficiency of MAP30-HBP but has a slight effect on its colocalization with lysosomes. This observation was further corroborated by analyzing the fluorescence signals obtained from the IPP software (Media Cybernetics Inc., Silver Spring, MD) and calculating the Pearson's correlation coefficient between FITC and LysoTracker signal positions⁴¹ (Figure 3B). The colocalization of MAP30-HBP with lysosomes decreased slightly after treatment with QBS, sodium aescinate, esculentoside A, phytolaccagenin, saikosaponin A, saikosaponin D, dipsacoside B, macranthoidin A, and CQ, respectively. No effect was observed with other saponins. Therefore, further verification by other methods is required to ascertain if the above saponins do possess endosomal escape activity.

3.3. Saponin-Mediated Augmentation of Cytotoxicity and Induction of Apoptosis by Endocytic Proteins. Like

most endocytic toxins, MAP30-HBP entrapped within endosomes must be released into the cytoplasm to exert its effect on cell growth inhibition. Therefore, saponin-mediated endosomal release of MAP30-HBP as reflected by enhanced cytotoxic effects was assessed in different cell types. MAP30-HBP (500, 100, 20, 4, and 0.8 nM) with or without different saponins at working and NCMIC concentrations (Table 1) were incubated with HeLa and SMMC-7721 cells. Cell viability was measured by the MTT assay after 24 h of incubation. Figures 4A and S6 show that cell proliferation was differentially suppressed by MAP30-HBP when it was coadministered with various saponins. The fold increase in inhibitory effects was calculated as the ratio of average IC_{50} values of the MAP30-HBP-treated group and the MAP30-HBP-/saponin-treated group, and the results are presented as a bar graph (Figure 4B). As shown in Figure 4B, sodium aescinate and QBS enhanced the cytotoxicity of MAP30-HBP more than 10^6 to 10^9 times.

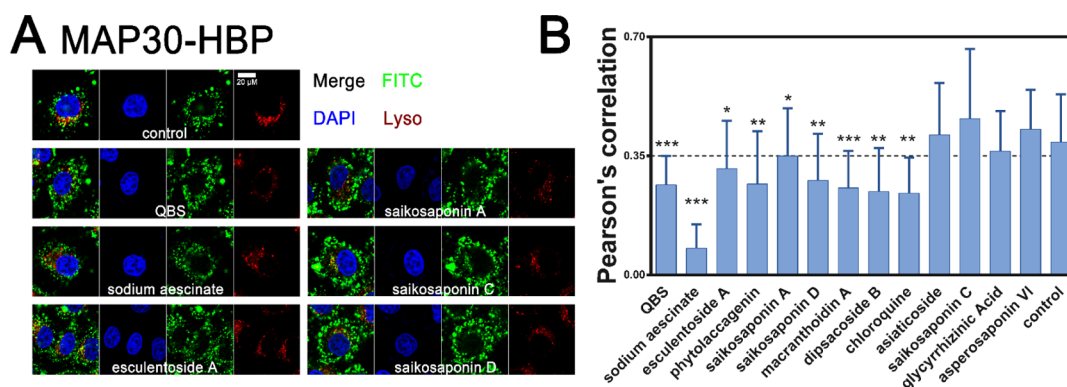


Figure 3. Effects of various saponins on translocation efficiency and colocalization of MAP30-HBP with lysosomes. HeLa cells were incubated with FITC-labeled MAP30-HBP (5 μ M) and different saponins for 2 h, costained with DAPI (blue) and LysoTracker (Red). Images were captured using confocal microscopy. Bar graph showing Pearson's coefficient values of colocalization between MAP30-HBP and lysosomes (each group contained about 20 individual cells). Error bars represent the mean \pm SD. * p < 0.05, ** p < 0.01, *** p < 0.001.

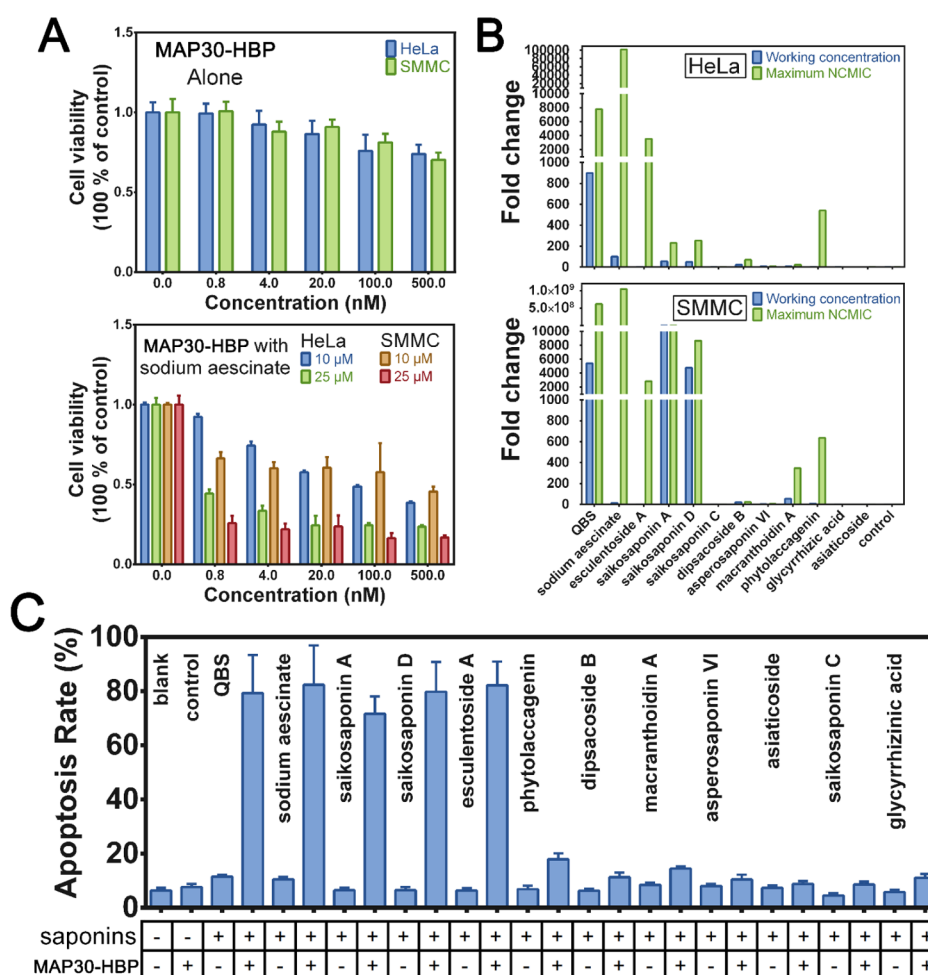


Figure 4. Effect of MAP30-HBP with saponins on cell viability and the induction of cell apoptosis. (A) HeLa and SMMC-7721 cells were incubated with MAP30-HBP and saponins, followed by the MTT assay, and the data were presented as mean \pm SD (N = 5). Cells treated with dialysis buffer (20 mM Tris-HCl/0.5 M NaCl/5% glycerol) with or without saponins served as controls. (B) The fold changes were calculated by dividing the IC_{50} value of the MAP30-HBP group with the IC_{50} value of the saponin-treated group. IC_{50} values of MAP30-HBP were calculated by GraphPad Prism 6.0 software. (C) SMMC-7721 cells were incubated with 5 nM MAP30-HBP with one of the 12 saponins, respectively. Cells were collected and stained with Annexin V-PE/7-AAD, followed by flow cytometry. The apoptosis rate (Q_2 + Q_3) was calculated by Flow Jo software and plotted by GraphPad 6.0 software. Data were presented as mean \pm SD, N = 3.

The fold increase of esculentoside A, saikosaponin A, and saikosaponin D was about 600–10 000 times. For macranthoidin A and dipsacoside B, the fold changes were about 10–

500 times. The other saponins did not show any significant enhancement effect on the cytotoxicity of MAP30-HBP. Analysis of apoptosis using the Annexin-V-PE/7-AAG

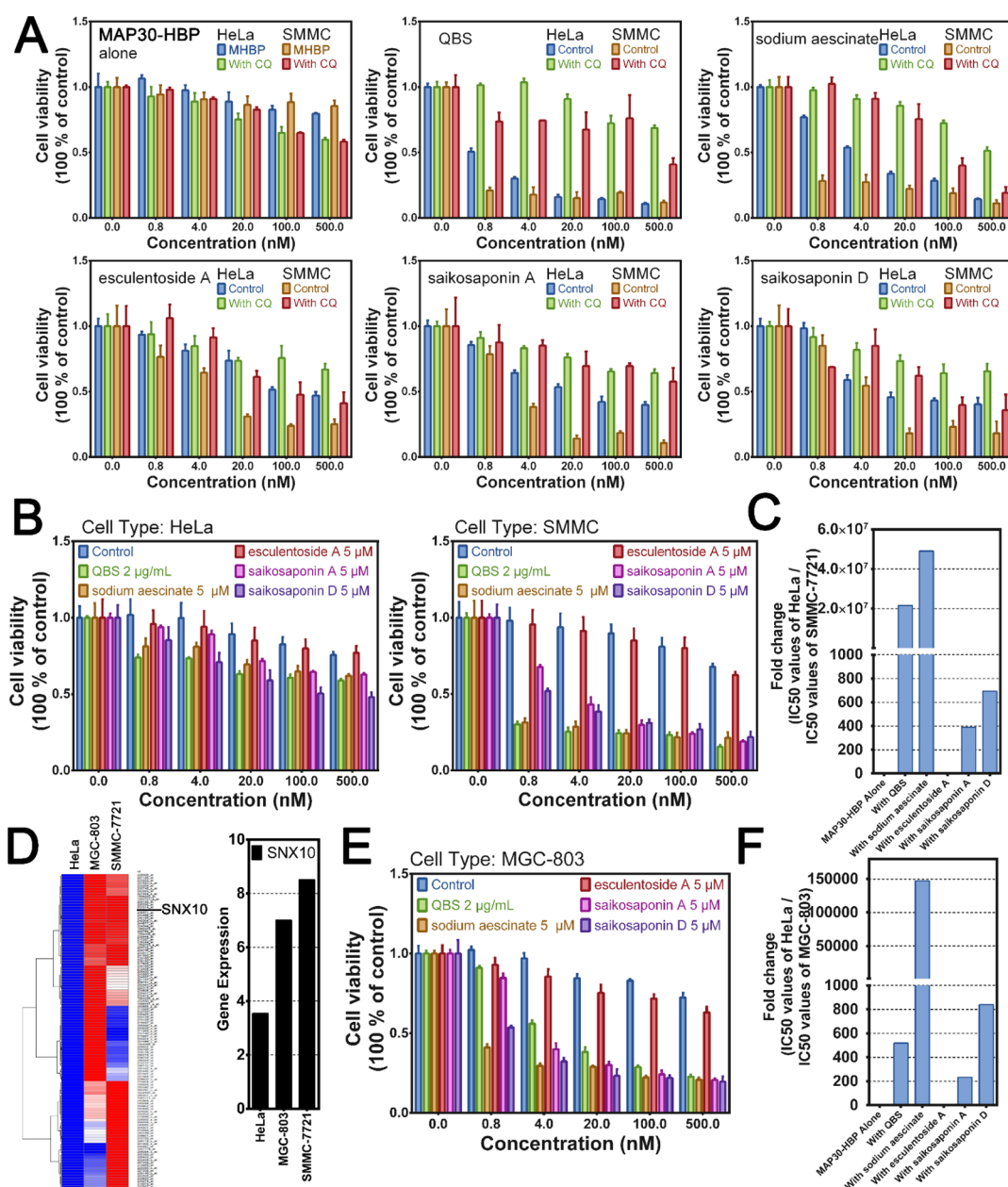


Figure 5. Saponin-mediated endosomal escape is inhibited by high lysosomal pH and exhibits cell-type dependency. (A) HeLa and SMMC-7721 cells were incubated with the derived working concentrations of each saponin for 24 h with or without 100 μ M CQ. Cell viability was measured using the MTT assay, and data were plotted using GraphPad 6.0 software. Error bars represent the mean \pm SD, $N = 5$. (B) HeLa and SMMC-7721 cells were incubated with MAP30-HBP alone (control) or MAP30-HBP with 2 μ g/mL QBS, 5 μ M sodium aescinate, 5 μ M esculentoside A, 5 μ M saikosaponin A, or 5 μ M saikosaponin D for 24 h, followed by the MTT assay. Data were presented as mean \pm SD, $N = 5$. (C) The fold changes between HeLa and SMMC-7721 cells were calculated by dividing the IC₅₀ values of HeLa with IC₅₀ values of SMMC-7721. (D) Gene expression array analysis between HeLa, SMMC-7721, and MGC-803 cells ($P < 0.001$ and fold change > 1.5). The SNX10 expression in SMMC-7721 and MGC-803 cells was 2.3 times more than in HeLa cells according to the gene expression analysis. (E) MGC-803 cells were incubated with MAP30-HBP alone (control) or MAP30-HBP with one of five different saponins for 24 h, followed by the MTT assay. Data were plotted using GraphPad 6.0 software, and the error bars represent the mean \pm SD, $N = 5$. (F) The fold changes between HeLa and MGC-803 cells were calculated by dividing the IC₅₀ values of HeLa with IC₅₀ values of MGC-803.

apoptosis kit showed that the increase in cytotoxicity was due to increased MAP30-HBP-mediated apoptosis in SMMC-7721 cells in the presence of active saponins such as QBS, sodium aescinate, esculentoside A, saikosaponin A, and saikosaponin D (Figure 4C).

Taken together, the results of the MTT assay, apoptosis analyses, and colocalization experiments led us to conclude that QBS, sodium aescinate, esculentoside A, saikosaponin A,

and saikosaponin D could modulate the intracellular distribution of MAP30-HBP, thereby significantly increasing the cytotoxicity of MAP30-HBP. In other words, among the 12 saponins tested, these 5 saponins displayed the strongest endosomal escape activity. Although dipsacoside B, macranthoidin A, and phytolaccagenin weakly inhibited colocalization with lysosomes, they only slightly enhanced the cytotoxicity of

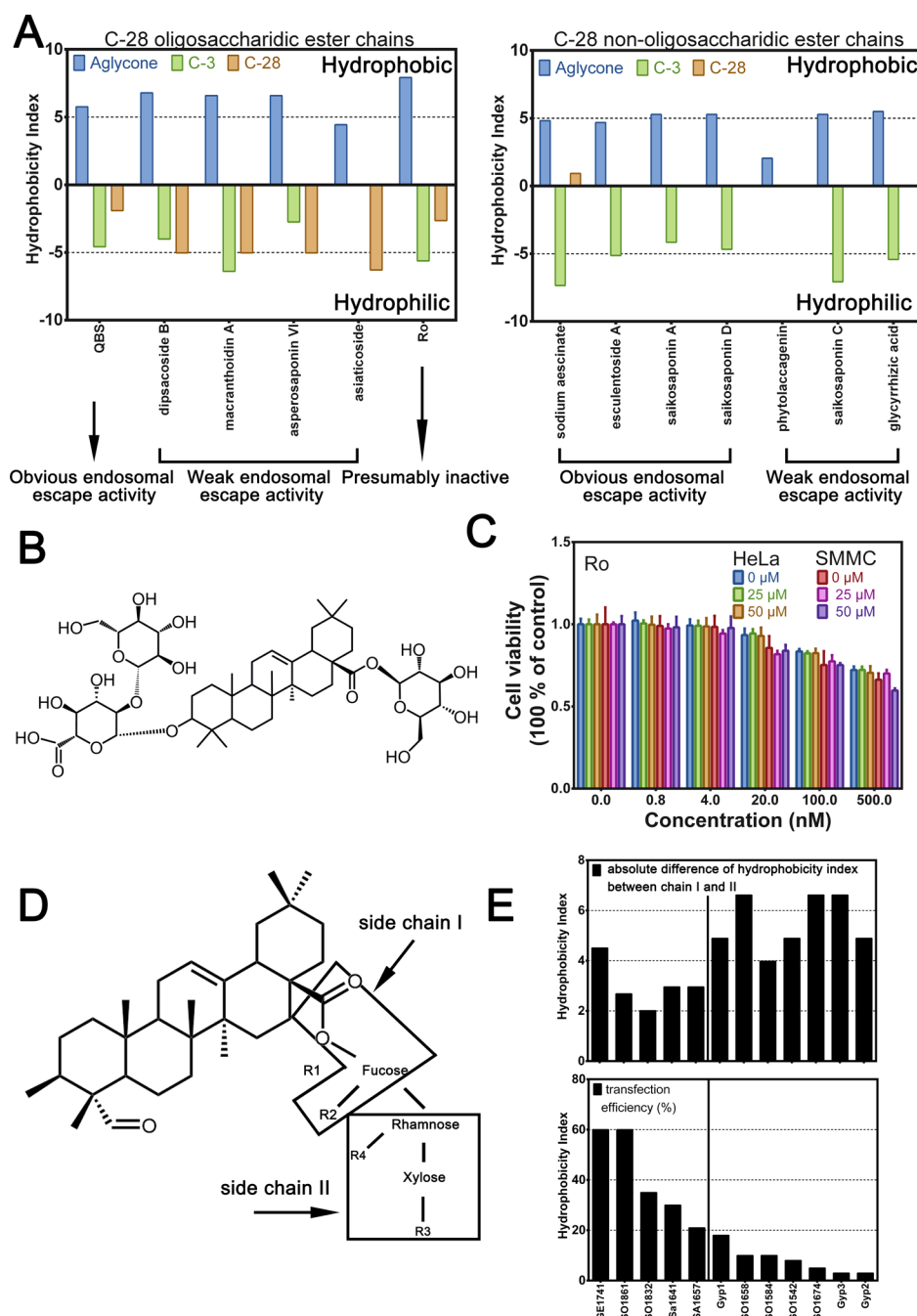


Figure 6. Analysis of saponin structure–activity relationship. (A) The hydrophobicity index of the aglycone, C-3, and C-28 side chains was calculated by JSME. (B) Structure of ginsenoside Ro. (C) HeLa and SMMC-7721 cells were incubated with MAP30-HBP and different concentrations (25, 50 μ M) of ginsenoside Ro for 24 h, followed by the MTT assay. Data were plotted using GraphPad 6.0 software, and the error bars represent the mean \pm SD, $N = 5$. (D) Structure of saponins with C-28 sugar chains. (E) The hydrophobicity index of side chain I and side chain II was calculated by JSME and plotted using GraphPad software.

MAP30-HBP, indicating moderate endosomal escape activity. The others manifested no obvious endosomal escape activity.

3.4. Saponin-Mediated Endosomal Escape Is Dependent on Cell-Type and Intra Vesicular pH. Next, we further sought to elucidate the potential mechanisms underlying the endosomal escape activity of the five potent saponins. Previous studies indicated that intra vesicular pH affects the endosomal escape activity of saponins.⁴² Therefore, the same experimental scheme using CQ to increase the pH of endosomes/lysosomes was employed to determine the effects of intra vesicular pH on saponin-mediated endosomal release

in cells. Different concentrations of MAP30-HBP were used to treat HeLa and SMMC-7721 cells for 24 h coadministered with selected saponins and 100 μ M CQ, followed by the MTT assay. Cytotoxicity of MAP30-HBP was significantly decreased in the presence of saponins and CQ but not with CQ alone (Figure 5A), suggesting that lysosomal acidification is involved in endosomal escape induced by saponins.

Interestingly, saponin-mediated endosomal release was cell-type-dependent, with enhanced cytotoxicity across the full range of MAP30-HBP concentrations in SMMC-7721 but not HeLa cells (Figures 4 and 5B). As shown in Figure 5B, QBS,

sodium aescinate, saikosaponin A, and saikosaponin D could significantly enhance the cytotoxicity of MAP30-HBP in SMMC-7721 cells (about 800 to 10^7 times), while only a slight enhancement effect could be seen in HeLa cells (about 4–30 times). No obvious endosomal escape was observed in the esculentoside A group possibly because of its relatively low endosomal escape efficiency at this concentration. The bar chart in Figure 5C which is derived by calculating the ratio of average IC_{50} values of HeLa and SMMC-7721 cells shows that the effect of saponin-mediated endosomal escape is cell-type-dependent.

To explain the cell-type dependency of the saponin-mediated endosomal release, we analyzed the gene expression profile of HeLa and SMMC-7721 from the NCBI GEO dataset contributed by Astra Zeneca (GEO accession GSE57083).³⁵ Phosphatidylinositol-3-monophosphate binding proteins contribute to multiple endosomal retrieval pathways.⁴³ In particular, it was found that the expression level of the sorting nexin 10 (SNX10) gene in SMMC-7721 cells was higher than that in HeLa cells (Figure 5D), leading us to suspect that cells with high endogenous levels of SNX10 are more responsive to saponin-mediated cytotoxicity enhancement of endocytosed MAP30-HBP. To corroborate this finding, we investigated the cytotoxicity of MAP30-HBP with saponins against another SNX10 high expression cell line MGC-803 and it was also found to be higher than HeLa cells (about 233 to 10^5 times), reflecting a similar response as in SMMC-7721 cells (Figure 5E,F).

3.5. Structure–Activity Relationship of Saponins. The 12 oleanane-type saponins differed in their ability to elicit endosomal release, and this property may be related to their structural features. Oleanane-type saponins are a class of typical detergent-like amphiphilic compounds with the same aglycone backbone. However, the side chains attached to the aglycone differ in polarity and can directly affect its endosomal escape activity. We listed the number and types of sugars attached to these saponins. Most saponins have a glucose moiety attached to C3 or C28. However, no clear pattern of correlation with endosomal escape activity could be found (Table S3). Therefore, we pursued a different approach to clarify the structure–activity relationship of saponins from another point of view. The online freeware JSME^{44,45} was used to calculate the hydrophobicity of the aglycone and key side chains. The values are then summarized and correlated with the determined endosomal escape activity of each saponin. The work of Böttger et al. showed that the C-3 and C-28 side chains on the aglycone have large effects on the activity of saponins.⁴⁶ Therefore, we used JSME to calculate the hydrophobic index of the C-3 and C-28 side chains as well as the aglycone backbone of all 12 saponins (Figure 6A). The 12 saponins may be divided into two groups on the basis of their C-28 side chain. Group I saponins (such as QBS and dipsacoside B) are those where the C-28 side chain comprises an acidic oligosaccharide ester chain. Group II saponins (e.g., saikosaponin A and esculentoside A) have a nonoligosaccharide or no side chain at the C-28 position. In previous studies, the endosomal escape activity of the glycosylated triterpene SO1861, which would fall under Group I in our classification scheme, has been attributed to the C-3 linked branched trisaccharide and the C-28 linked branched sugar chain.³¹ However, our experimental data showed that Group I saponins such as dipsacoside B and macranthoidin A did not exert strong endosomal escape activity even at 100 μ M (Figure 4B).

Comparing these saponins with those that contain C-28 oligosaccharidic ester chains, it could be concluded that it is the C-4 aldehyde group that contributed to the strong endosomal escape activity of Group I saponins (Figure 1), which was consistent with previous findings.^{33,46} For saponins with no side C-28 chains such as saikosaponin A and saikosaponin D, those exhibiting strong endosomal escape activity have a hydrophilic C-3 side chain (the hydrophobicity index of between -5 and 0). If there were nonoligosaccharidic chains bound to C-28 such as sodium aescinate, the C-28 side chain should be hydrophobic (the hydrophobicity index was above 0).

We also used these proposed rules to predict whether a candidate saponin has endosomal escape activity. Ginsenoside Ro is a typical oleanane-type saponin and was used to test our hypothesis. As shown in Figure 6A,B, both C-3 and C-28 bound sugar chains of ginsenoside Ro were hydrophilic and no aldehyde group was attached to C-4, portending poor endosomal escape activity. Subsequent MTT assay revealed that no enhancement of MAP30-HBP could be observed in the presence of ginsenoside Ro, which is concordant with our proposed prediction rules (Figure 6C).

Melzig et al. carefully analyzed the effects of the sugar side chain attached on C-28 of saponin on the endosomal escape activity. They showed that the lipophilic character of the C-28 sugar side chain and the hydrophilicity of the sugars attached to xylose of the C-28 chain affected the endosomal escape activity.³¹ We also calculated the hydrophobic index of the C-3 and C-28 side chains of the saponins used in their studies but found no clear pattern of correlation with endosomal escape activity (Figure S7). Considering the importance of different C-28 sugar side chains, further detailed analysis led us to divide the carbohydrate moiety into two parts, side chain I (fucose) and side chain II (Figure 6D), and then calculate their hydrophobic index values. It can be concluded that when the hydrophobic index between chain I and chain II of the C-28 side chain has a smaller absolute difference (Figure 6E) (less than 4.5), then it is more likely that the saponin will exhibit significant endosomal escape activity (such as GE1741, SO1861, SO1832, and SA1641).

4. DISCUSSION

Although CPPs can successfully solve the transmembrane delivery problem of most in vivo administered protein drugs, the release of protein drugs from endosomes to the cytosol remains a major obstacle that greatly limits their therapeutic potency. Different approaches have been used to release internalized drugs into the cytosol, for example, by means of fusion with natural EEDs of microbial origin or by coadministering protein drugs with small molecules that prevent the conversion of endosomes to lysosomes, such as CQ, or EEEs that facilitate the spontaneous escape of protein drugs from the endosomes. Previous studies have indicated the limited efficacy of EED in eliciting cytosolic release. While the endosome escape enhancement effect of EEE is more pronounced than that of EED, the former also has its own unique limitations.¹³

Recently, a unique class of medicinal plant saponins which have been used for centuries in traditional Chinese medicine for the treatment of various diseases has been discovered to have strong endosomal escape activities.²⁴ Although the available data have been focused on only a few saponins, such as SO1861, their efficacy is very impressive.⁴² The

structure of saponins is complex and diverse, and the number of saponins reported to exhibit endosomal escape effects is currently small. Hence, structure–activity relationships remain unclear, giving rise to the motivation of this study to elucidate structural features that are associated with strong endosomal escape activity and to shed light on the underlying mechanisms. Of the 12 medicinal plant saponins studied, 5 were found to exhibit strong endosomal escape activity at NCMIC when coadministrated with MAP30-HBP. These saponins reduced the accumulation of internalized MAP30-HBP protein in lysosomes and enhanced the cytotoxicity of MAP30-HBP by promoting cell apoptosis in a pH- and cell-type-dependent manner. Exceptional enhancement of MAP30-HBP cytotoxicity was elicited by QBS and sodium aescinate with 10^6 to 10^9 fold increase in cell death, compared with the modest 10-fold increase observed with CQ.

It is noteworthy that the cytotoxic enhancement effect of saponin on MAP30-HBP cytotoxicity in SMMC-7721 cells is more pronounced than in HeLa cells. The IC_{50} values of MAP30-HBP in SMMC-7721 and HeLa cells were almost the same, while in the presence of saponins, the growth inhibition effect of MAP30-HBP in SMMC-7721 cells was several thousand times higher than in HeLa cells. This phenomenon suggests that saponin-mediated endosomal escape was cell-type-dependent and is associated with high expression of endogenous SNX10 as revealed by the analysis of microarray-based gene expression profiling data (GSE57803). This finding is further corroborated by similar responses in another high SNX10-expressing cell line, MGC-803. Interestingly, SNX10 activity has been shown to induce vacuolation in mammalian cells and may play an important role in endosome homeostasis.⁴⁷ In fact, sorting nexins are responsible for cellular protein trafficking⁴⁸ and are involved in multiple endosomal retrieval pathways.⁴³ In addition, the cytotoxicity of Type 1 RIPs such as MAP30 has been demonstrated to be enhanced via transportation to the endoplasmic reticulum (ER) by means of conjugation with an ER-targeting KDEL peptide.^{49,50} This suggests that intracellular transportation of internalized toxins should be taken into account when assessing the efficacy of protein drugs. In particular, SNX10 was found to be highly expressed in cervical squamous cell carcinoma and endocervical adenocarcinoma (CESC) (Figure S8A), and CESC patients with high SNX10 expression also showed a poorer overall survival (Figure S8B) using web server GEPIA.⁵¹ It is tantalizing to speculate that dual administration of MAP30-HBP and saponins could possibly be more effective in cancers expressing high levels of SNX10, presenting a potentially powerful tool for increased efficacy and specificity in oncotherapy.

Recently, the structure and properties of C-28 branched sugar side chains have been associated with the endosomal escape activity of different saponins.³¹ However, the work focused on several saponins ($MW \geq 1.6$ kD) with similar side-chain structures, and no data for saponins without C-28 sugar side chains were available from the study. Our study showed that saponins with no side chain at the C-28 position and hydrophobicity index of the C-3 side chain between -5 and 0 could exert strong endosomal escape activity, such as saikosaponin A and saikosaponin D. Saponins with non-oligosaccharidic chains bound to C-28 whereby the C-28 side chains were hydrophobic (hydrophobicity index >0) could exert strong endosomal escape activity such as sodium aescinate. Saponins without C-28 branched sugar side chains

and smaller molecule mass ($MW \leq 1.4$ kD) can also exert high endosomal escape activity.

Additionally, a previous study demonstrated the key positive contribution of the aldehyde group at C-4 in eliciting the endosomal escape activity of saponins,²⁴ and this phenomenon was also observed in our study where QBS with a C-4 aldehyde also exhibited strong endosomal escape activity. It is possible that this characteristic of the C-28 side chain affects the amphiphilic structure of the entire saponin, thereby affecting the endosomal escape activity. Taken together, we propose some simple rules based on specific structural characteristics to predict if a saponin has significant endosomal escape activity:

- I. For those saponins without a C-28 side chain, the hydrophobicity index of the C-3 side chain should be within -5 to 0 ;
- II. For those saponins with a C-28 nonsugar side chain, this side chain should be hydrophobic and a C-4 aldehyde group is also needed;
- III. For those saponins with a C-28 sugar chain and C-4 aldehyde group, the C-28 branched sugar side chain I and chain II should have similar hydrophobicity (the absolute difference of hydrophobicity index is less than 4).

Further work will be required to validate the proposed rules.

■ ASSOCIATED CONTENT

Supporting Information

The Supporting Information is available free of charge at <https://pubs.acs.org/doi/10.1021/acs.molpharmaceut.9b01158>.

Information about the structure of QBS, cytotoxicity of 12 saponins on HeLa and SMMC-7721 cells, purification of recombinant proteins, effect of MAP30-HBP with saponins on cell viability, analysis of saponin structure–activity relationship, impact of SNX10 expression on overall patient survival with CESC; list of 11 saponins identified in QBS; and overview of the tested saponins in terms of structure (PDF)

■ AUTHOR INFORMATION

Corresponding Authors

Fu-Jun Wang — Zhejiang Fonow Medicine Company, Ltd., Dongyang, China, Shanghai R&D Center for Standardization of Chinese Medicines, Shanghai, China, and Shanghai University of Traditional Chinese Medicine, Shanghai, China; orcid.org/0000-0002-4914-6006; Email: wfj@shutcm.edu.cn; Fax: +86 21 51322508

Jian Zhao — East China University of Science and Technology, Shanghai, China; orcid.org/0000-0003-1574-5331; Email: zhaojian@ecust.edu.cn; Fax: +86 21 64252257

Other Authors

Xue-Wei Cao — East China University of Science and Technology, Shanghai, China

Oi-Wah Liew — Centre for Translational Medicine, Singapore

Ye-Zhou Lu — East China University of Science and Technology, Shanghai, China

Complete contact information is available at:

<https://pubs.acs.org/10.1021/acs.molpharmaceut.9b01158>

Notes

The authors declare no competing financial interest.

ACKNOWLEDGMENTS

The authors declare that they have no conflict of interest regarding the conduct or outcomes of this study. This work was supported by the National Natural Science Foundation of China (grant no. 81571795) and Natural Science Foundation of Shanghai (grant no. 19ZR1457300). The authors are grateful to Ji-Yue Kang and Wei Wang of the Department of Applied Biology for assistance with the preparation of recombinant proteins. The authors also thank Ting Wu and Bo-Hao Yu at Research Center of Analysis and Test for help on confocal microscopy. The authors are also grateful to Li Zhou of the State Key Laboratory of Bioreactor Engineering for assistance with flow cytometry analyses.

REFERENCES

- (1) Fawell, S.; Seery, J.; Daikh, Y.; Moore, C.; Chen, L. L.; Pepinsky, B.; Barsoum, J. Tat-Mediated Delivery of Heterologous Proteins into Cells. *Proc. Natl. Acad. Sci. U.S.A.* **1994**, *91*, 664–668.
- (2) Jones, A. T. Macropinocytosis: Searching for an Endocytic Identity and Role in the Uptake of Cell Penetrating Peptides. *J. Cell Mol. Med.* **2007**, *11*, 670–684.
- (3) Mayor, S.; Pagano, R. E. Pathways of Clathrin-Independent Endocytosis. *Nat. Rev. Mol. Cell Biol.* **2007**, *8*, 603–612.
- (4) Madani, F.; Lindberg, S.; Langel, U.; Futaki, S.; Gräslund, A. Mechanisms of Cellular Uptake of Cell-Penetrating Peptides. *J. Biophys.* **2011**, *2011*, 1.
- (5) Erazo-Oliveras, A.; Najjar, K.; Dayani, L.; Wang, T.-Y.; Johnson, G. A.; Pellois, J.-P. Protein Delivery into Live Cells by Incubation with an Endosomolytic Agent. *Nat. Methods* **2014**, *11*, 861–867.
- (6) LeCher, J. C.; Nowak, S. J.; Mcmurry, J. L. Breaking in and Busting out: Cell-Penetrating Peptides and the Endosomal Escape Problem. *Biomol. Concepts* **2017**, *8*, 131–141.
- (7) Shete, H. K.; Prabhu, R. H.; Patravale, V. B. Endosomal Escape: A Bottleneck in Intracellular Delivery. *J. Nanosci. Nanotechnol.* **2014**, *14*, 460–474.
- (8) Hetzel, C.; Bachran, C.; Fischer, R.; Fuchs, H.; Barth, S.; Stöcker, M. Small Cleavable Adapters Enhance the Specific Cytotoxicity of a Humanized Immunotoxin Directed against CD64-Positive Cells. *J. Immunother.* **2008**, *31*, 370–376.
- (9) Neundorff, I.; Rennert, R.; Hoyer, J.; Schramm, F.; Löbner, K.; Kitanovic, I.; Wölfl, S. Fusion of a Short HA2-Derived Peptide Sequence to Cell-Penetrating Peptides Improves Cytosolic Uptake, but Enhances Cytotoxic Activity. *Pharmaceutics* **2009**, *2*, 49–65.
- (10) Chignola, R.; Anselmi, C.; Serra, M. D.; Franceschi, A.; Fracasso, G.; Pasti, M.; Chiesa, E.; Lord, J. M.; Tridente, G.; Colombatti, M. Self-Potential of Ligand-Toxin Conjugates Containing Ricin A Chain Fused with Viral Structures. *J. Biol. Chem.* **1995**, *270*, 23345–23351.
- (11) Liou, J.-S.; Liu, B. R.; Martin, A. L.; Huang, Y.-W.; Chiang, H.-J.; Lee, H.-J. Protein Transduction in Human Cells Is Enhanced by Cell-Penetrating Peptides Fused with an Endosomolytic HA2 Sequence. *Peptides* **2012**, *37*, 273–284.
- (12) Michiue, H.; Tomizawa, K.; Wei, F.-Y.; Matsushita, M.; Lu, Y.-F.; Ichikawa, T.; Tamiya, T.; Date, I.; Matsui, H. The NH2 Terminus of Influenza Virus Hemagglutinin-2 Subunit Peptides Enhances the Antitumor Potency of Polyarginine-Mediated p53 Protein Transduction. *J. Biol. Chem.* **2005**, *280*, 8285–8289.
- (13) Fuchs, H.; Weng, A.; Gilabert-Oriol, R. Augmenting the Efficacy of Immunotoxins and Other Targeted Protein Toxins by Endosomal Escape Enhancers. *Toxins* **2016**, *8*, 200.
- (14) Andersson, Y.; Engebraaten, O.; Fodstad, Ø. Synergistic Anti-Cancer Effects of Immunotoxin and Cyclosporin in Vitro and in Vivo. *Br. J. Cancer* **2009**, *101*, 1307–1315.
- (15) Wu, Y. N.; Gadina, M.; Tao-Cheng, J. H.; Youle, R. J. Retinoic Acid Disrupts the Golgi Apparatus and Increases the Cytosolic Routing of Specific Protein Toxins. *J. Cell Biol.* **1994**, *125*, 743–753.
- (16) Griffin, T.; Raso, V. Monensin in Lipid Emulsion for the Potentiation of Ricin A Chain Immunotoxins. *Cancer Res.* **1991**, *51*, 4316–22.
- (17) Griffin, T. W.; Childs, L. R.; Fitzgerald, D. J.; Levin, L. V. Enhancement of the Cytotoxic Effect of Anti-Carcinoembryonic Antigen Immunotoxins by Adenovirus and Carboxylic Ionophores. *J. Natl. Cancer Inst.* **1987**, *79*, 679.
- (18) Colombatti, M.; Dell'Arciprete, L.; Chignola, R.; Tridente, G. Carrier Protein-Monensin Conjugates: Enhancement of Immunotoxin Cytotoxicity and Potential in Tumor Treatment. *Cancer Res.* **1990**, *50*, 1385–1391.
- (19) Handa, J. T.; Houston, L. L.; Jaffe, G. J. Monensin Enhances the Cytotoxic Effect of Antitransferrin Receptor Immunotoxin on Cultured RPE Cells. *Curr. Eye Res.* **1993**, *12*, 45–53.
- (20) Casellas, P.; Bourrie, B. J.; Gros, P.; Jansen, F. K. Kinetics of Cytotoxicity Induced by Immunotoxins. Enhancement by Lysosomotropic Amines and Carboxylic Ionophores. *J. Biol. Chem.* **1984**, *259*, 9359–9364.
- (21) Lizzi, A. R.; D'Alessandro, A. M.; Zeolla, N.; Brisdelli, F.; D'Andrea, G.; Pitari, G.; Oratore, A.; Bozzi, A.; Ippoliti, R. The Effect of AZT and Chloroquine on the Activities of Ricin and a Saporin-transferrin Chimeric Toxin. *Biochem. Pharmacol.* **2005**, *70*, 560–569.
- (22) Song, Z.-T.; Zhang, L. W.; Fan, L. Q.; Kong, J. W.; Mao, J. H.; Zhao, J.; Wang, F. J. Enhanced Anticancer Effect of MAP30-S3 by Cyclosporin A through Endosomal Escape. *Anticancer Drugs* **2018**, *29*, 736–747.
- (23) Bachran, D.; Schneider, S.; Bachran, C.; Urban, R.; Weng, A.; Melzig, M. F.; Hoffmann, C.; Kaufmann, A. M.; Fuchs, H. Epidermal Growth Factor Receptor Expression Affects the Efficacy of the Combined Application of Saponin and a Targeted Toxin on Human Cervical Carcinoma Cells. *Int. J. Cancer* **2010**, *127*, 1453–1461.
- (24) Fuchs, H.; Niesler, N.; Trautner, A.; Sama, S.; Jerz, G.; Panjideh, H.; Weng, A. Glycosylated Triterpenoids as Endosomal Escape Enhancers in Targeted Tumor Therapies. *Biomedicines* **2017**, *5*, 14.
- (25) Szakiel, A.; Pączkowski, C.; Henry, M. Influence of Environmental Abiotic Factors on the Content of Saponins in Plants. *Phytochem. Rev.* **2011**, *10*, 471–491.
- (26) Sparg, S. G.; Light, M. E.; van Staden, J. Biological Activities and Distribution of Plant Saponins. *J. Ethnopharmacol.* **2004**, *94*, 219–243.
- (27) Bachran, C.; Sutherland, M.; Heisler, I.; Hebestreit, P.; Melzig, M. F.; Fuchs, H. The Saponin-Mediated Enhanced Uptake of Targeted Saporin-Based Drugs Is Strongly Dependent on the Saponin Structure. *Exp. Biol. Med.* **2006**, *231*, 412–420.
- (28) Gilabert-Oriol, R.; Furness, S. G. B.; Stringer, B. W.; Weng, A.; Fuchs, H.; Day, B. W.; Kourakis, A.; Boyd, A. W.; Hare, D. L.; Thakur, M.; et al. Dianthin-30 or Gelonin versus Monomethyl Auristatin E, Each Configured with an Anti-Calcitonin Receptor Antibody, Are Differentially Potent in Vitro in High-Grade Glioma Cell Lines Derived from Glioblastoma. *Cancer Immunol. Immunother.* **2017**, *66*, 1217–1228.
- (29) Bhargava, C.; Dürkop, H.; Zhao, X.; Weng, A.; Melzig, M. F.; Fuchs, H. Targeted Dianthin Is a Powerful Toxin to Treat Pancreatic Carcinoma When Applied in Combination with the Glycosylated Triterpene SO1861. *Mol. Oncol.* **2017**, *11*, 1527–1543.
- (30) Thakur, M.; Weng, A.; Bachran, D.; Riese, S. B.; Böttger, S.; Melzig, M. F.; Fuchs, H. Electrophoretic Isolation of Saponin Fractions from Saponinum Album and Their Evaluation in Synergistically Enhancing the Receptor-Specific Cytotoxicity of Targeted Toxins. *Electrophoresis* **2011**, *32*, 3085–3089.
- (31) Sama, S.; Jerz, G.; Thakur, M.; Melzig, M.; Weng, A. Structure–Activity Relationship of Transfection-Modulating Saponins

- A Pursuit for the Optimal Gene Trafficker. *Planta Med.* **2019**, *85*, 513–518.

(32) Thakur, M.; Weng, A.; Pieper, A.; Mergel, K.; von Mallinckrodt, B.; Gilbert-Oriol, R.; Görick, C.; Wiesner, B.; Eichhorst, J.; Melzig, M. F.; et al. Macromolecular Interactions of Triterpenoids and Targeted Toxins: Role of Saponins Charge. *Int. J. Biol. Macromol.* **2013**, *61*, 285–294.

(33) Melzig, M. F.; Hebestreit, P.; Gaidi, G.; Lacaille-Dubois, M. A. Structure–activity- relationship of saponins to enhance toxic effects of agrostin. *Planta Med.* **2005**, *71*, 1088–1090.

(34) Luo, Z.; Cao, X. W.; Li, C.; Wu, M. D.; Yang, X. Z.; Zhao, J.; Wang, F. J. The heparin-binding domain of HB-EGF as an efficient cell-penetrating peptide for drug delivery. *J. Pept. Sci.* **2016**, *22*, 689–699.

(35) Wappett, M. Expression Data from AstraZeneca Internal Cell Lines, GSE57083. <https://www.ncbi.nlm.nih.gov/geo/query/acc.cgi?acc=GSE57083>, 2014.

(36) Augustin, J. M.; Kuzina, V.; Andersen, S. B.; Bak, S. Molecular Activities, Biosynthesis and Evolution of Triterpenoid Saponins. *Phytochemistry* **2011**, *72*, 435–457.

(37) Sioud, M.; Mobergslén, A. Selective Killing of Cancer Cells by Peptide-Targeted Delivery of an Anti-Microbial Peptide. *Biochem. Pharmacol.* **2012**, *84*, 1123–1132.

(38) Weng, A.; Thakur, M.; Beceren-Braun, F.; Bachran, D.; Bachran, C.; Riese, S. B.; Jenett-Siems, K.; Gilbert-Oriol, R.; Melzig, M. F.; Fuchs, H. The Toxin Component of Targeted Anti-Tumor Toxins Determines Their Efficacy Increase by Saponins. *Mol. Oncol.* **2012**, *6*, 323–332.

(39) Lee-Huang, S.; Huang, P. L.; Chen, H.-C.; Huang, P. L.; Bourinbaia, A.; Huang, H. I.; Kung, H.-f. Anti-HIV and Anti-Tumor Activities of Recombinant MAP30 from Bitter Melon. *Gene* **1995**, *161*, 151–156.

(40) Lee-Huang, S.; Huang, P. L.; Nara, P. L.; Chen, H.-C.; Kung, H.-f.; Huang, P.; Huang, H. I.; Huang, P. L. MAP 30: A New Inhibitor of HIV-1 Infection and Replication. *FEBS Lett.* **1990**, *272*, 12–18.

(41) Han, K.; Zhu, J.-Y.; Jia, H.-Z.; Wang, S.-B.; Li, S.-Y.; Zhang, X.-Z.; Han, H.-Y. Mitochondria-Targeted Chimeric Peptide for Trinitarian Overcoming of Drug Resistance. *ACS Appl. Mater. Interfaces* **2016**, *8*, 25060–25068.

(42) Weng, A.; Thakur, M.; Von Mallinckrodt, B.; Beceren-Braun, F.; Gilbert-Oriol, R.; Wiesner, B.; Eichhorst, J.; Böttger, S.; Melzig, M. F.; Fuchs, H. Saponins Modulate the Intracellular Trafficking of Protein Toxins. *J. Control. Release* **2012**, *164*, 74–86.

(43) Cullen, P. J.; Korswagen, H. C. Sorting Nexins Provide Diversity for Retromer-Dependent Trafficking Events. *Nat. Cell Biol.* **2012**, *14*, 29–37.

(44) White, B.; Perna, I.; Carlson, R. Software for Teaching Structure-Hydrophobicity Relationships. *Biochem. Mol. Biol. Educ.* **2005**, *33*, 65–70.

(45) Bienfait, B.; Ertl, P. JSME: A Free Molecule Editor in JavaScript. *J. Cheminf.* **2013**, *5*, 24.

(46) Böttger, S.; Westhof, E.; Siems, K.; Melzig, M. F. Structure-Activity Relationships of Saponins Enhancing the Cytotoxicity of Ribosome-Inactivating Proteins Type I (RIP-I). *Toxicon* **2013**, *73*, 144–150.

(47) Qin, B.; He, M.; Chen, X.; Pei, D. Sorting Nexin 10 Induces Giant Vacuoles in Mammalian Cells. *J. Biol. Chem.* **2006**, *281*, 36891–36896.

(48) Chen, Y.; Wu, B.; Xu, L.; Li, H.; Xia, J.; Yin, W.; Li, Z.; Shi, D.; Li, S.; Lin, S.; et al. A SNX10/V-ATPase Pathway Regulates Ciliogenesis in Vitro and in Vivo. *Cell Res.* **2012**, *22*, 333–345.

(49) Stirpe, F.; Battelli, M. G. Ribosome-Inactivating Proteins: Progress and Problems. *Cell. Mol. Life Sci.* **2006**, *63*, 1850–1866.

(50) Nakatsu, K.; Hosoi, T.; Toyoda, K.; Ozawa, K. Synthesis of a Peptide That Can Translocate to the Endoplasmic Reticulum. *Biochem. Biophys. Res. Commun.* **2015**, *460*, 628–632.

(51) Tang, Z.; Li, C.; Kang, B.; Gao, G.; Li, C.; Zhang, Z. GEPIA: A Web Server for Cancer and Normal Gene Expression Profiling and Interactive Analyses. *Nucleic Acids Res.* **2017**, *45*, W98–W102.